Clinical Cancer Research

VEGFR1$^+$ Metastasis–Associated Macrophages Contribute to Metastatic Angiogenesis and Influence Colorectal Cancer Patient Outcome

Aida Freire Valls[1,2], Karl Knipper[1], Evangelia Giannakouri[3,4], Víctor Sarachaga[2], Sascha Hinterkopf[1], Michael Wuehrl[1], Ying Shen[1], Praveenkumar Radhakrishnan[1], Johannes Klose[1], Alexis Ulrich[1], Martin Schneider[1], Hellmut G. Augustin[3,4], Carmen Ruiz de Almodovar[2,4,5], and Thomas Schmidt[1]

Abstract

Purpose: To investigate the clinical relevance of macrophages in liver metastasis of colorectal cancer and their influence on angiogenesis and patient survival. Moreover to evaluate specific blood monocytes as markers of disease recurrence.

Experimental design: In a mouse model with spontaneous liver metastasis, the angiogenic characteristics of tumor- and metastasis (MAM)-associated macrophages were evaluated. Macrophages and the vasculature from 130 primary tumor (pTU) and 123 patients with liver metastasis were assessed. *In vivo* and in human samples, the clinical relevance of macrophage VEGFR1 expression was analyzed. Blood samples from patients ($n = 157$, 80 pTU and 77 liver metastasis) were analyzed for assessing VEGFR1-positive (VEGFR1$^+$) cells as suitable biomarkers of disease recurrence.

Results: The number of macrophages positively correlated with vascularization in metastasis. Both in the murine model as well as in primary isolated human cells, a subpopulation of MAMs expressing VEGFR1 were found highly angiogenic. While VEGFR1 expression in pTU patients did not predict prognosis; high percentage of VEGFR1$^+$ cells in liver metastasis was associated with worse patient outcome. Interestingly, VEGFR1$^+$-circulating monocytes in blood samples from patients with liver metastasis not only predicted progression but also site of recurrence.

Conclusions: Our findings identify a new subset of proangiogenic VEGFR1$^+$ MAMs in colorectal cancer that support metastatic growth and may become a liquid biomarker to predict disease recurrence in the liver.

Introduction

Despite early detection and improvements in treatment, colorectal cancer is still the third most common cause of death among all cancer entities (1). Overall survival (OS) is reduced in patients diagnosed with metastases (2), highlighting the need to improve our understanding of the metastatic process. While the principles of the metastatic cascade are of interest, a deeper understanding of the growth of established metastasis is of vital importance for finding new therapeutic targets and improving patients' welfare. As more than two thirds of colorectal cancer metastases are found in the liver (2), we focused our study on understanding how macrophages can influence angiogenesis and growth of liver metastasis and thereby influence patient outcome.

Macrophages can exert pro- or antitumorigenic effects (3, 4) in the tumor microenvironment and play various roles in each step of disease progression. Accordingly, several studies exist with contradictory findings about the correlation of macrophages with patient survival and disease recurrence. While tumor-associated macrophages (TAMs) have been described to act more antitumorigenic in primary colorectal cancer (5, 6), metastasis-associated macrophages (MAMs) have not yet been well characterized. In this study, we hypothesized that TAMs and MAMs have different angiogenic potentials.

Within the multifaceted features of macrophages, one important role is the induction of angiogenesis, a hallmark of cancer (7, 8). Hypoxia drives VEGF upregulation in tumors leading to the development of blood vessels from preexisting ones (9). In primary colorectal cancer tumors, VEGF expression correlates positively with the occurrence of liver metastasis. Likewise, vessel density was found to negatively influence OS in metastatic patients (10). VEGF binds to its tyrosine kinase receptors, the VEGFRs, expressed ubiquitously in the tumor microenvironment. In the monocyte/macrophage lineage, VEGF signals via VEGFR1 which recruits macrophages from bone marrow to the tumor (11, 12) and influences metastatic initiation and

[1]Department of General, Visceral, and Transplantation Surgery, University Hospital of Heidelberg, Heidelberg, Germany. [2]Biochemistry Center Heidelberg (BZH), Heidelberg University, Heidelberg, Germany. [3]Division of Vascular Oncology and Metastasis, German Cancer Research Center (DKFZ), Heidelberg, Germany. [4]European Center for Angioscience (ECAS), Medical Faculty Mannheim, Heidelberg University, Heidelberg, Germany. [5]Institute for Transfusion Medicine and Immunology, Medical Faculty Mannheim, Heidelberg University, Mannheim, Germany.

Note: Supplementary data for this article are available at Clinical Cancer Research Online (http://clincancerres.aacrjournals.org/).

A. Freire Valls and K. Knipper contributed equally to this article.

Corresponding Author: Thomas Schmidt, Heidelberg University, Im Neuenheimer Feld 110, Heidelberg 69120, Germany. Phone: 4962-2156-6111; Fax: 4962-2156-5506; E-mail: thomas1.schmidt@med.uni-heidelberg.de

Clin Cancer Res 2019;25:5674–85

doi: 10.1158/1078-0432.CCR-18-2123

Translational Relevance

While complete surgical resection of metastases in colorectal cancer can prolong patient survival, disease recurrence still remains a clinical problem. Even though the introduction of antiangiogenic therapy resulted in prolonged survival, in many cases resistance mechanisms develop. Currently it remains unclear how metastatic angiogenesis in colorectal cancer liver metastases is regulated. Moreover, a biomarker that detects early recurrence and is practicable in clinical use remains to be found. Here, we first identified VEGFR1-positive (VEGFR1$^+$) metastasis associated macrophages as contributors to angiogenesis in liver metastasis both in humans and in a clinically relevant liver metastasis mouse model. Furthermore, we observed that VEGFR1$^+$-circulating monocytes from blood of patients with liver metastasis correlate with progression-free survival and site of disease recurrence. Altogether, we have characterized VEGFR1$^+$-circulating cells as promising biomarkers of disease recurrence in patients with metastatic colorectal cancer.

growth (13, 14). In the liver, VEGFR1-positive (VEGFR1$^+$) macrophages have been shown to infiltrate hypoxia-driven injured areas via the peripheral blood (15). Moreover, in the context of VEGF/VEGFR inhibition, macrophage depletion further suppressed tumor growth and hence, highlights their value on regulating disease outcome (16). In this study we evaluated the role of VEGFR1$^+$ macrophages in liver metastasis of colorectal cancer.

As prediction of disease recurrence after metastatic liver resection remains a clinical challenge, we also evaluated VEGFR1$^+$ macrophages as liquid biopsy to assess patients' risk profiles after surgical interventions. Several clinical and biological features have been identified as prognostic factors of colorectal cancer relapse, including tumor markers in the blood (17, 18). Also, advances on the genetic characterization of tumors resulted in promising assays, which correlate with OS of patients with colorectal liver metastasis, but still can only be assessed in resected tumor tissue (19). Therefore, a noninvasive method that could be used would be desirable.

In summary, the aim of this study was to elucidate the role of macrophages in liver metastasis angiogenesis and patient outcome. Our results reveal VEGFR1$^+$ MAMs as highly angiogenic and predictors of progression-free survival (PFS). Moreover, we found a new prognostic marker of relapse as circulating VEGFR1$^+$ monocytes in blood of patients with liver metastasis correlated with PFS and site of disease recurrence.

Materials and Methods

Patients

A total of 210 patients diagnosed with primary colorectal carcinoma (pTU) and 200 patients diagnosed with colorectal liver metastasis were included in this study (Supplementary Table S1). All patients underwent surgery between 2007 and 2017 at the Department of General, Visceral and Transplantation Surgery of the University Hospital Heidelberg (Heidelberg, Germany). From 37 patients, both the pTU and the liver metastasis were analyzed, which had synchronous liver metastasis at the time of surgery (Supplementary Table S1, synchronous). Our study was approved by the Ethics Committee of the Medical Faculty Heidelberg and was conducted in accordance with the declaration of Helsinki. Written informed consent was obtained from all enrolled patients. Patient data were collected prospectively. Tumor tissue samples of 93 patients with pTU and 123 patients with liver metastasis were obtained for IHC purposes (Supplementary Table S1). Venous blood samples were obtained from 80 patients with pTU and 77 patients with liver metastasis (Supplementary Table S1; flow cytometry). Of the patients with liver metastasis, 64.9% received neoadjuvant therapy (Supplementary Table S2). Tumor and nontumor tissue samples of 13 patients with pTU and 17 patients with liver metastasis were obtained for cell isolation by magnetic cell separation in 2016/2017.

IHC and immunofluorescence

Stainings were performed following an in-house protocol (20). Further details are specified in the Supplementary Data.

Murine model of metastatic colorectal cancer

All experimental protocols of mice were approved and performed in accordance to local authorities and animal welfare officers of Baden-Wuerttemberg, Germany. All mice were cared for in accordance with the "Guide for the Care and Use of Laboratory Animals" by the National Academy of Sciences. A highly metastatic cell line was established by positive selection as described previously (21). Cells were infected with luciferase-expressing lentiviral premade particles (Ambiso). Tumor and metastatic growth were evaluated using bioluminescence imaging. Briefly, 200 μL of Beetle luciferin (15 mg/mL in water; Promega) were intraperitoneally injected in anesthetized mice. After 5 minutes, bioluminescent images were acquired using the IVIS Imaging System (Xenogen).

Cell culture and sprouting assay

Cell culture was performed as described previously (20, 22). Fibrin gel sprouting assays were performed as described previously (23). Further details are specified in the Supplementary Data.

Magnetic cell separation

Freshly collected tissues, both from mouse and human, were used for isolation of CD11b$^+$ cells as described previously (5). For both, murine CD11b$^+$ and CD11b$^+$/F4/80$^+$ isolation prior to MACS separation, cells were applied onto a Percoll Gradient (Sigma-Aldrich). Cells were incubated with F4/80-biotin antibody (clone REA126, 1:10; Miltenyi Biotec) for 15 minutes at 4°C. Then, cells were incubated with streptavidin microbeads for 15 minutes at 4°C (1:10; Miltenyi Biotec). F4/80$^+$ cell populations were isolated and then incubated with CD11b MicroBeads (clone M1/70.15.11.5, 1:10; Miltenyi Biotec) for 15 minutes at 4°C. After application into MS Columns, the CD11b$^+$/F4/80$^+$ cell populations were obtained.

Flow cytometry and FACS

Single-cell suspensions from murine pTU and liver metastasis were prepared as described for magnetic cell separation. Cells were incubated with F4/80-FITC (clone A3-1, 1:20; AbD Serotec) in flow cytometry buffer (eBioscience). Then, for M1 and M2 staining, cells were fixed with IC Fixation Buffer (Thermo Fisher

Scientific) for 20 minutes at room temperature, permeabilized with Permeabilization Buffer (Thermo Fisher Scientific) and stained in this buffer with Nos2-PerCP (clone N20, 1:50; Santa Cruz Biotechnology) and CD206-BV421 (clone C068C, 1:50; BioLegend) for 30 minutes at room temperature, respectively. For sorting TAMs and MAMs, fresh single-cell suspensions were also stained with CD11b-PE (clone M1/70.15.11.5, 1:10; Miltenyi Biotec). $CD11b^+/F4/80^+$ macrophages were sorted with BD FACSAria III sorter directly into RLT Buffer (Qiagen), for RNA isolation. Murine blood was also stained with CD45-PerCP (Clone 30-F11, 1:100, BD Bioscience). Cells from human blood samples were incubated with CD11b-PE (clone M1/70.15.11.5, 1:10; Miltenyi Biotec) for 30 minutes at 4°C. Afterward, fixation and permeabilization was performed as before. CD68 (clone 298807, 1:20; R&D Systems) and VEGFR1 (Y103, 1:100; Abcam) were used for 30 minutes at room temperature. Appropriate secondary antibodies were incubated for 30 minutes at room temperature (1:500; Thermo Fisher Scientific). For all samples, negative and corresponding IgG controls were additionally performed. Data were acquired with a BD FACSCanto II Flow Cytometer (BD Biosciences). Analysis was performed with FlowJo 10.4.2 (FlowJo, LLC).

RNA isolation and gene expression analysis by qRT-PCR

RNA isolation of macrophages was performed with the RNeasy MiniKit (Qiagen) following the manufacturer's instructions with a DNA digestion step using the RNase-Free DNase Set (Qiagen). For sorted cells, to reverse transcribe RNA samples to cDNA, SuperScript VILO cDNA Synthesis Kit (Invitrogen) was used. qRT-PCR was performed using Fast SYBR Green Master Mix (Thermo Fisher Scientific). *ActB* was used as internal control. All qPCR results were obtained from at least three biological repeats. Primers used are listed in Supplementary Table S3.

Lentiviral production

Plasmids containing the miRNA control and miRNA against Flt1 were generated using the BLOCK-iT Pol II miR RNAi Expression Vector Kit (Invitrogen) following the manufacturer's instructions. Then, validated miRNAs were cloned in the pLVTHM plasmid vector expressing GFP for generating the lentivirus. Lentiviruses were produced by transfection of HEK293-T cells by the calcium phosphate method with the corresponding vectors. Lentivirus-containing supernatants were collected 72 hours after transfection and concentrated by ultracentrifugation at 22,000 rpm for 90 minutes at 4°C.

Transduction of hematopoietic stem cells and tumor injection

Hematopoietic stem cells were obtained with the Lineage Cell Depletion Kit (Miltenyi Biotec) following the manufacturer's instructions. Cells were harvested from Balbc/J mice and cultured in StemSpan SFEM Medium (Stemcell Technologies; supplemented with 50 ng/mL mSCF, mTPO, and Flt3-L; R&D Systems) and 1% penicillin-streptomycin and glutamine for 24 hours. Then, cells were plated in a RetroNectin (TaKaRa, 20 μg/mL) coated plate and transduced with lentiviruses containing either the control miRNA or the miRNA against Flt1 with 4 μg/mL polybrene (Thermo Fisher Scientific). After 48 hours, GFP-positive cells were sorted. For lethal irradiation, receptor mice were irradiated twice with 3.5 Gy and 200,000 cells per mouse were injected in the tail vein. After 4 weeks, tumors were implanted in the mice as before.

Isolation of white blood cell fraction

Venous peripheral blood samples were collected in EDTA tubes. The white blood cell fraction was isolated by a density gradient centrifugation with Histopaque-1077 (Sigma-Aldrich). Erythrocytes were lysed by Red Blood Cell Lysis Buffer (Roche). The collected cells were frozen at −80°C with DMSO (Sigma-Aldrich).

Statistical analysis

All values shown are mean ± SEM, if not differently stated. To calculate statistical significance, the two-tailed Student *t* test (when comparing two groups) or one-way ANOVA with Bonferroni multiple comparisons test (when comparing three or more groups) were used in Prism software. For correlation analysis, D'Agostino–Pearson omnibus normality test was performed to evaluate Gaussian distribution and accordingly, correlation was evaluated either with two-tailed Pearson correlation test or nonparametric Spearman correlation test in Prism software. Statistical significance was taken as $P < 0.05$. OS was measured from time of surgery until death or loss of follow-up, and PFS was measured from time of surgery until loss of follow-up or disease recurrence. Disease recurrence was assessed by cross-sectional imaging. For grouping of the patients' medians for von Willebrand Factor (vWF; 2.1% in pTU, 1.95% in liver metastasis, and 1.99% and 1.97% in synchronous pTU and liver metastasis, respectively), CD68 staining (114 cells/mm^2 in pTU, 116 cells/mm^2 in liver metastasis, and 124 cells/mm^2 and 80 cells/mm^2 in synchronous pTU and liver metastasis, respectively) and VEGFR1 (167 cells/mm^2 in pTU, 117 cells/mm^2 in liver metastasis, and 173 cells/mm^2 and 124 cells/mm^2 in synchronous pTU and liver metastasis, respectively) were calculated and patients were grouped as low <2% or high >2% vessel density or as low <100 cells/mm^2 or high >100 cells/mm^2 macrophage infiltration or the median itself for VEGFR1, accordingly. Kaplan–Meier method and log-rank test was used for survival analysis. Results for PFS were confirmed with multivariate Cox regression analysis. Statistical analyses were performed with SPSS Statistics 24.0 (IBM).

Results

A subset of MAMs expresses high Flt1 and are more angiogenic than TAMs

Within the tumor stroma, macrophages have the ability to rapidly polarize (3). As we hypothesized that TAMs and MAMs have different proangiogenic properties, we first characterized macrophage polarization. To do so, we used a traceable orthotopic CT26 colon cancer mouse model forming primary tumors in the cecum (pTU) that spontaneously metastasize to the liver in almost 90% of the mice (Fig. 1A and B). A simple but useful classification of M1-like [proinflammatory, nitric oxide synthase (NOS_2)-positive] and M2-like (anti-inflammatory, proangiogenic, mannose receptor (MR)-positive] polarized macrophages has been broadly used (24). We used the cell surface marker F4/80 (murine-specific macrophage marker) together with NOS_2 and MR to characterize the TAM and MAM activation phenotype by flow cytometry (Fig. 1C and D). Our results showed that pTUs had

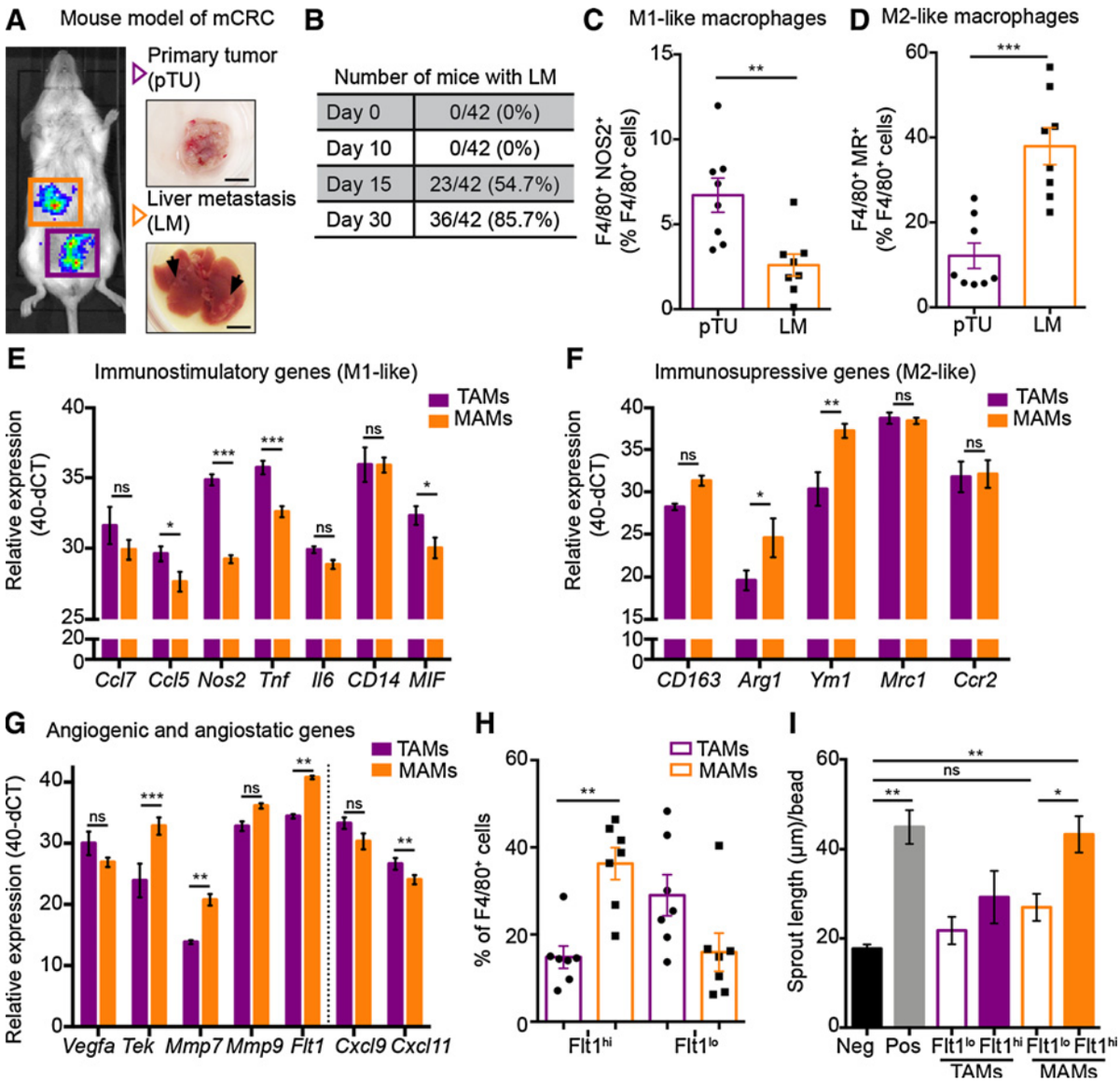

Figure 1.

MAMs are skewed toward an M2-like phenotype, express Flt1, and are highly angiogenic. **A,** Mouse model of metastatic colorectal cancer. Bioluminescence image of a mouse injected with luciferase-expressing CT26 cells and corresponding dissected tissue showing a primary tumor (pTU, purple square) and liver metastasis (LM, orange square). Arrows point to macroscopic liver metastasis. **B,** Supplementary Table showing the number of mice with liver metastasis after tumor injection, measured by positive bioluminescent signal at the indicated days. Quantification of flow cytometry analysis for M1-like (F4/80$^+$/Nos2$^+$; **C**) and M2-like (F4/80$^+$/MR$^+$; **D**) macrophages ($n = 8$; two-tailed unpaired Student *t* test; **, $P < 0.01$; ***, $P < 0.001$). qRT-PCR of F4/80$^+$/Cd11b$^+$-sorted TAMs and MAMs showing that TAMs express M1-like genes (**E**), while MAMs express M2-like genes (**F**; normalized to β-actin, relative expression calculated as 40-dCT). Includes immunostimulatory genes for M1 characterization (**E**); includes immunosuppressive genes for M2 (**F**). **G,** qRT-PCR of F4/80$^+$/Cd11b$^+$-sorted TAMs and MAMs showing that MAMs express high levels of *Flt1.* Angiogenic genes are *Vegfa, Tek, Mmp7, Mmp9, and Flt1.* Angiostatic genes are *Cxcl9* and *Cxcl11* (normalized to β-actin, relative expression calculated as 40-dCT); for **E–G**, $n = 4$ (two-way ANOVA with Bonferroni multiple comparison test *, $P < 0.05$; **, $P < 0.01$; ***, $P < 0.001$; ns: not significant). **H,** Quantification of F4/80$^+$/Flt1^{lo} and F4/80$^+$/Flt1^{hi} macrophages in pTU and liver metastasis showing an increase of Flt1^{hi} macrophages in liver metastasis ($n = 7$; two-tailed unpaired Student *t* test; **, $P < 0.01$). **I,** Quantification of endothelial cell sprouting showing that Flt1^{hi} MAMs are more angiogenic than Flt1^{lo} MAMs and TAMs. Starvation medium as negative control (Neg) and VEGF (50 ng/mL) as positive control (Pos). $n = 3$; one-way ANOVA; *, $P < 0.05$; **, $P < 0.01$; ns: not significant). Scale bar, 5 mm (**A**).

a 2.5-fold higher M1-like (F4/80$^+$/Nos2$^+$) macrophage infiltration than liver metastasis ($P = 0.005$; Fig. 1C). Conversely, a 3-fold higher infiltration of M2-like macrophages (F4/80$^+$/MR$^+$) was observed in liver metastasis ($P < 0.001$; Fig. 1D).

For further characterization, we used the general myeloid marker CD11b and the F4/80 to FACS TAMs and MAMs from pTU and liver metastasis (Supplementary Fig. S1A). Consistently, qPCR-based expression analyses revealed that TAMs exhibited a

M1-like immunostimulatory polarization in contrast to MAMs, while MAMs showed a more M2-like immunosuppressive polarization (Fig. 1E and F).

To address the angiogenic potential of TAMs and MAMs, we isolated CD11b$^+$ cells from liver metastasis or pTUs by magnetic separation and generated conditioned medium (CM) to stimulate endothelial cells in sprouting assays. Liver metastasis MAM-derived CM was able to significantly induce sprouting angiogenesis (3.2-fold; $P < 0.001$), while TAM-derived CM induced angiogenesis to a lower extend (1.6-fold; $P = 0.079$;Supplementary Fig. S1B and S1C).

As it was recently shown that Flt1 (VEGFR1 in humans) is highly expressed by a subset of macrophages that support breast cancer metastasis (13) and as Flt1 signaling in myeloid cells can support tumor angiogenesis (25), we investigated the expression of Flt1 in MAMs. Indeed, qPCR analyses of sorted TAMs and MAMs showed a significant upregulation of *Flt1* in MAMs (78.8-fold change; $P < 0.001$; Fig. 1G). Moreover, we found that MAMs express higher levels of known proangiogenic genes such as *Tek*, encoding for the tyrosine kinase receptor Tie2 (26). In contrast, we observed that Cxcl11, an angiostatic chemokine, is highly expressed by TAMs (Fig. 1G). By flow cytometry and immunofluorescence on isolated macrophages, we confirmed that MAMs express more FLT1 than TAMs also at protein levels (Fig. 1H; $P < 0.01$; Supplementary Fig. S1D; and Supplementary Fig. S1E and S1F; $P < 0.001$).

Furthermore, to address the functional relevance of Flt1^{hi} MAMs, we sorted CD11b$^+$ F4/80$^+$ Flt1^{hi} or Flt1^{lo} MAMs and TAMs and performed sprouting assays (Fig. 1I; Supplementary Fig. S1G). Interestingly, our results showed that Flt1^{hi} MAMs were highly angiogenic (2.4-fold increase, compared with negative control; $P < 0.01$), while Flt1^{hi} and Flt1^{lo} TAMs and Flt1^{lo} MAMs were not. As Flt1^{hi} TAMs did not induce sprouting angiogenesis, we analyzed whether they were still more M1-like polarized. Indeed, Flt1^{hi} TAMs express more *Nos2* than Flt1^{hi} MAMs and significantly less *Flt1* (Supplementary Fig. S1H).

In summary, these results indicate that Flt1^{hi} MAMs have a proangiogenic role in the liver metastatic microenvironment.

Bone marrow knockdown of Flt1 reduces liver metastasis and its vascularization

To address the relevance of Flt1 expression in macrophages in metastatic angiogenesis, we knocked down Flt1 in hematopoietic stem cells. Lineage-depleted bone marrow cells were transduced with a GFP-expressing lentiviral vector containing a miRNA against Flt1 or control. GFP$^+$ control bone marrow cells (miR-Ctrl) or Flt1-knocked down cells (miR-Flt1) were transplanted into irradiated mice. Four weeks after bone marrow transplantation, CT26 colon tumors were injected in the cecum and after 3 weeks, knockdown efficiency, tumor growth, and angiogenesis were evaluated (Supplementary Fig. S2A). Survival analysis showed that three of eight mice in the control group died versus one of nine mice in the knockdown group (Supplementary Fig. S2B).

Mouse and liver weight were not different at the end of the experiment (Supplementary Fig. S2C and S2D). Also, primary tumor weight was not different (Fig. 2A). Interestingly, evaluation of liver metastases revealed a reduction of size in the miR-Flt1 group (1.4-fold reduction; $P = 0.038$; Fig. 2B; Supplementary Fig. S2E). Reduced FLT1 expression was confirmed at protein level in CD11b$^+$ cells from bone marrow (Fig. 2C; Supplementary Fig. S2F), as well as in blood (Fig. 2D; Supplementary Fig. S2G). qPCR analysis of sorted CD11b$^+$ cells revealed a significant *Flt1* reduction in blood (4.8-fold change; $P = 0.029$) and bone marrow (3.4-fold change; $P < 0.001$; Fig. 2E and F). Interestingly, a significant reduction of the proangiogenic metalloprotease 9 (*Mmp9*) expression in CD11b$^+$ bone marrow cells was also observed after Flt1 knockdown (3.0-fold change; $P < 0.01$), while other genes such *Vegfa* or *Tek* were not affected (Fig. 2F).

We further evaluated the vasculature of both primary tumors and liver metastasis by staining for platelet endothelial cell adhesion molecule (CD31) and the lymphatic vessel endothelial hyaluronan receptor 1 (Lyve1), which, besides the lymphatic vasculature, mainly labels hepatic blood sinusoidal endothelial cells in the liver (27). Quantification revealed that depletion of Flt1 (miR-Flt1) did not affect vessel density of the pTU but reduced vessel density by 58.7% ± 80% in liver metastasis (Fig. 2G–I).

These results show that Flt1^{hi} myeloid cells are able to support metastatic growth and angiogenesis in colorectal cancer.

Macrophage infiltration, VEGFR1 expression, and vessel density correlate with PFS in patients with colorectal cancer liver metastasis

Because we identified a proangiogenic macrophage subpopulation in mice, we assessed by IHC whether macrophage infiltration (CD68, human macrophage marker) within the tumor microenvironment correlated with vessel density (vWF, human vasculature marker) in patients diagnosed with colorectal cancer (Supplementary Table S1). Macrophage infiltration did not correlate with vascular density in pTU (Fig. 3A and B), while it did in liver metastasis (Fig. 3C and D), supporting that macrophages are more proangiogenic in liver metastasis than in pTU.

Then, to elucidate whether VEGFR1$^+$ macrophages in human colorectal cancer could also contribute to metastatic angiogenesis, we correlated the infiltration of VEGFR1$^+$ cells with vessel density in pTU and liver metastasis. Interestingly, no correlation of VEGFR1$^+$ cells with vessel density was observed in pTU samples (Fig. 3E and F), while a significant positive correlation was found in liver metastasis (Fig. 3G and H).

Analysis of tumor macrophage infiltration and vessel density showed no significant impact on OS (Supplementary Fig. S3A and S3B) or PFS of pTU patients (Fig. 3I and J); while known variables such as the International Union Against Cancer (UICC) staging or levels of circulating carcinoembryonic antigen (CEA) negatively influenced PFS and OS, respectively (UICC stage ≥ 3; HR, 5.280; $P = 0.003$/CEA ≥ 2.5 μg/L; HR, 2.609; $P = 0.043$).

While known parameters predicted reduced OS in patients with liver metastasis [Memorial Sloan Kettering Cancer Center (MSKCC) score ≥ 3; HR, 1.760; $P = 0.008$/CEA ≥ 200 μg/L; HR, 2.140; $P = 0.027$], neither macrophage infiltration nor vessel density had an impact on OS (Supplementary Fig. S3C and S3D). However, both high macrophage infiltration and high vessel density predicted reduced PFS in patients with liver metastasis (Fig. 3K and L).

In line, we observed that VEGFR1 staining did not predict OS in pTU (Supplementary Fig. S3E), nor in liver metastasis (Supplementary Fig. S3F). VEGFR1 also did not impact PFS in the pTU (Fig. 3M), but high infiltration in liver metastasis was associated to a reduced PFS (Fig. 3N).

We confirmed all the above-mentioned results in pTU and liver metastasis from patients with synchronous liver metastasis where

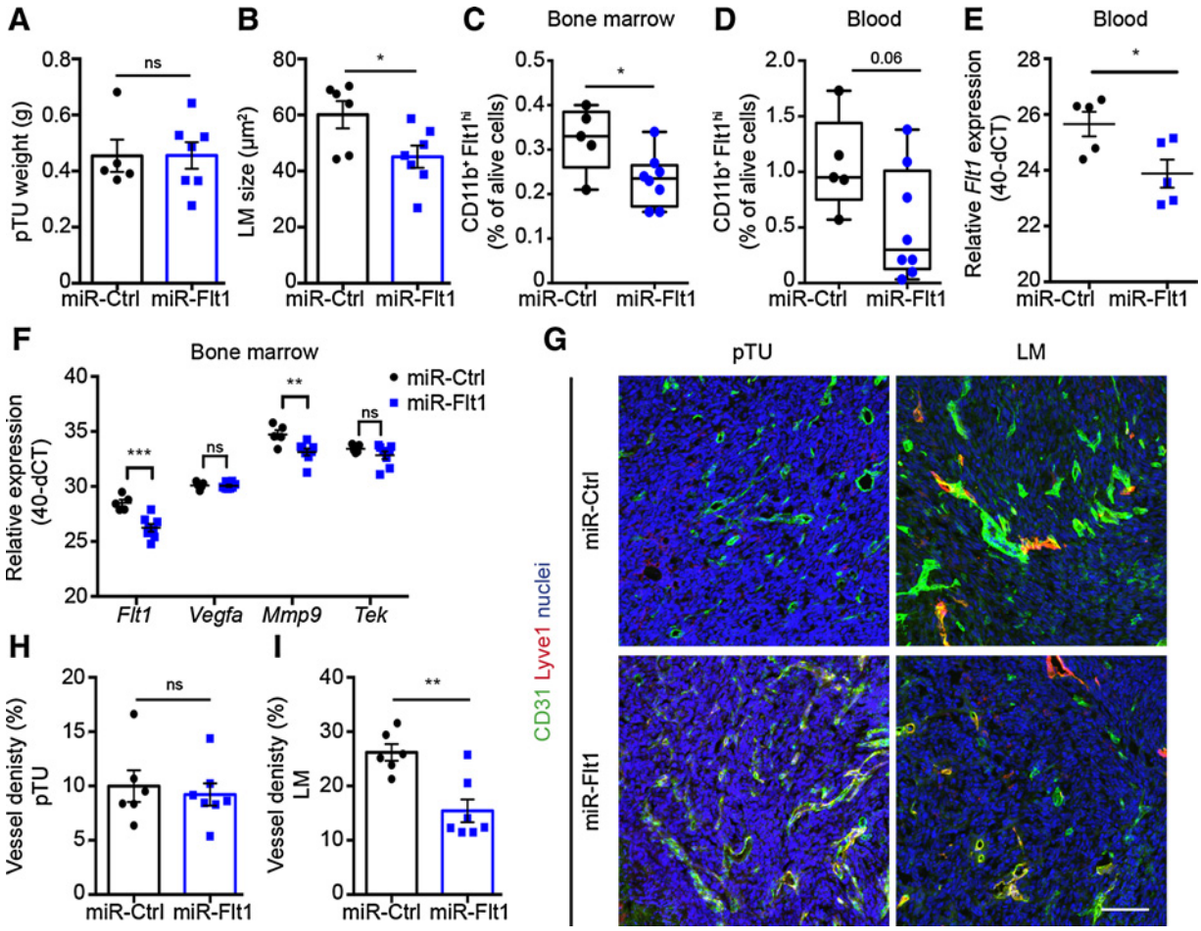

Figure 2.

Flt1^{hi} cells support liver metastasis growth and angiogenesis. **A,** Weight of primary tumors ($n = 5/7$; miR-ctrl/miR-Flt1). **B,** Quantification of the liver metastasis size showing that metastasis of the miR-Flt1 group are smaller compared with control; ($n = 6/7$; miR-Ctrl/miR-Flt1). Flow cytometry analysis of FLT1 expression of bone marrow (**C**) and blood (**D**) CD11b$^+$ showing a reduction of Flt1-expressing cells in the miR-Flt1 group ($n = 5/8$; miR-Ctrl/miR-Flt1). **E,** Relative Flt1 expression of CD11b$^+$-sorted cells from blood ($n = 5$). **F,** Relative expression of proangiogenic genes including *Flt1, Vegfa, Mmp9*, and *Tek* in bone marrow CD11b$^+$-sorted cells showing that miR-Flt1-transduced cells have a significantly reduced *Flt1* and *Mmp9* expression ($n = 5/6$; miR-Ctrl/miR-Flt1; two-way ANOVA with Bonferroni multiple comparisons test; **, $P < 0.01$; *** $P < 0.001$; ns: not significant). **G,** Immunofluorescence staining showing the vasculature (CD31/Lyve1 – general vascular markers) in the pTU and liver metastasis. Quantification of the CD31$^+$/Lyve1$^+$ area in both pTU (**H**) and liver metastasis (**I**) showing that depletion of Flt1 only affects liver metastasis vascularization ($n = 6/7$; miR-Ctrl/miR-Flt1). For **B**–**E**, **H**, and **I**, two-tailed unpaired Student *t* test; *, $P < 0.05$; **, $P < 0.01$; ns: not significant). Scale bar, 100 µm (**G**).

matched pairs of the pTUs and liver metastasis exist in the same patient (Supplementary Fig. S4A–S4P; Supplementary Table S1).

In summary, these results show that in human colorectal cancer liver metastases, vessel density and macrophage infiltration are prognostic factors of PFS and suggest that, VEGFR1$^+$ MAMs may contribute positively to angiogenesis.

Human MAMs express VEGFR1 and are proangiogenic

To elucidate the angiogenic potential of human macrophages, CM of freshly isolated human CD11b$^+$ cells after surgical resection of primary tumors or liver metastasis was used for sprouting angiogenesis assays. By immunofluorescence, we confirmed that VEGFR1$^+$ macrophages were present within the isolated CD11b$^+$ cells from the liver metastasis and the surrounding "no tumor" liver (ntL), and from the pTU and the surrounding "no tumor" mucosa (Mu). Indeed, there were 20% more VEGFR1$^+$ MAMs within the metastasis than in the surrounding tissue and 50% more than in the pTU (Fig. 4A and B). CD11b$^+$ MAMs were able to induce angiogenesis to a higher extend with more and longer endothelial cell sprouts than those in the surrounding liver and more than TAMs (Fig. 4C–E; 3-fold increase compared with negative control; $P < 0.001$).

In summary, we identified a subset of MAMs in human colorectal cancer that express VEGFR1 and are proangiogenic.

Circulating VEGFR1$^+$ monocytes in patients with liver metastasis predict disease recurrence

As Flt1$^+$ macrophages have been shown to be recruited to the metastatic site from the circulation (14, 25), we investigated whether VEGFR1$^+$ monocytes were present in the blood of patients with colorectal cancer liver metastasis (Supplementary Table S1).

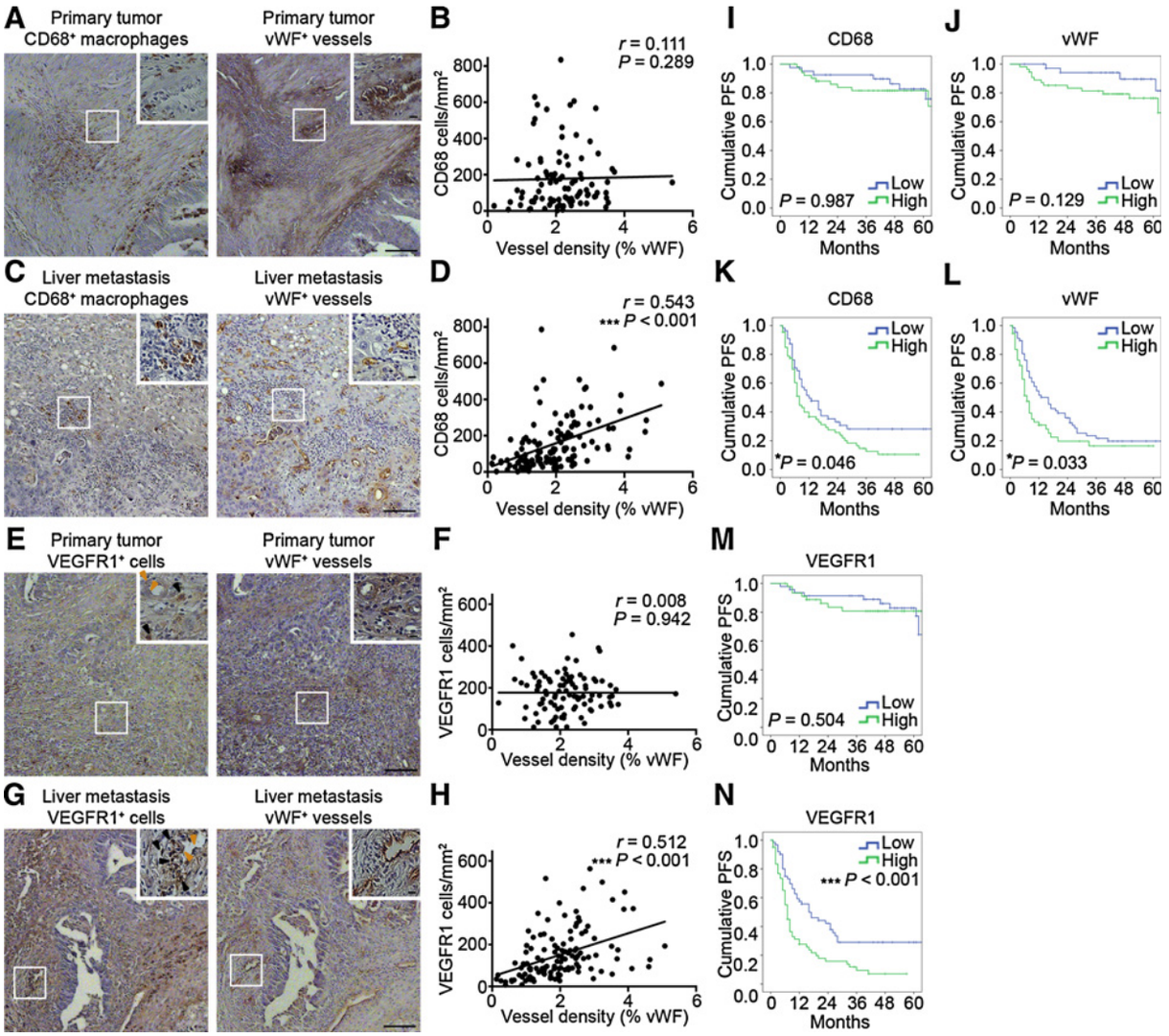

Figure 3.

Macrophage density and VEGFR1 expression correlate with vessel density and influence PFS in patients with liver metastasis of colorectal cancer. **A,** Representative images of macrophage (CD68) and vessel (vWF) IHC staining in primary colorectal cancer tumor samples (pTU). **B,** Correlation of the number of macrophages ($CD68^+$ cells/mm^2) and vessel density (% vWF) in pTU samples ($n = 93$). Spearman correlation coefficient (95% CI, −0.101–0.313). **C,** Representative images in colorectal cancer liver metastasis samples as in **A**. **D,** Correlation in liver metastasis samples ($n = 123$) as in **B**. Spearman correlation coefficient (95% CI, 0.400–0.660). **E,** Representative IHC images of VEGFR1 and vessel density (vWF) in pTU. Black arrows point to $VEGFR1^+$ macrophages, orange arrows to $VEGFR1^+$ endothelial cells (EC). **F,** Correlation of the number of $VEGFR1^+$-infiltrating cells (cells/mm^2) and vessel density (% vWF) in pTU samples ($n = 93$). Spearman correlation coefficient (95% CI, −0.202–0.217). **G,** Representative images of VEGFR1 and vessel (vWF) staining in colorectal cancer liver metastasis. Black arrows point to $VEGFR1^+$ macrophages, orange arrows to $VEGFR1^+$ ECs. **H,** Correlation of the number of $VEGFR1^+$-infiltrating cells (cells/mm^2) and vessel density (% vWF) in liver metastasis samples ($n = 123$). Pearson correlation coefficient (95% CI, 0.363–0.635). Kaplan–Meier survival curves showing PFS of pTU patients according to high ($n = 52$) or low ($n = 41$) $CD68^+$ cell infiltration (**I**) and according to high ($n = 55$) or low ($n = 38$) vessel density (**J**). Kaplan–Meier curves showing PFS of patients with liver metastasis according to $CD68^+$ cell infiltration [**K**; n (high) = 67, n (low) = 56] and vessel density [**L**; n (high) = 56, n (low) = 67]. Kaplan–Meier survival curves showing PFS according to $VEGFR1^+$ cell infiltration in pTU [**M**; n (high) = 46 or n (low) = 47] or in liver metastasis [**N**; n (high) = 61, n (low) = 62]. For all survival curves log-rank P value is shown. Scale bars (**A**, **C**, **E**, and **G**), overview, 100 μm; inset, 50 μm.

We performed flow cytometry analysis of human blood from patients with pTU or liver metastasis. We stained for CD11b (myeloid cell marker), CD68 (macrophage marker), and VEGFR1 on 77 liver metastasis and 80 pTU patients (Supplementary Fig. S5A–S5D). These patients were either diagnosed with liver metastasis or had a pTU, which was resected at the day of blood collection. Results showed no differences in percentage of circulating $CD11b^+/CD68^+$ monocytes ($P = 0.34$) or $VEGFR1^+$ ($P = 0.65$) cells between the different cohorts (Supplementary Fig. S5E–S5G).

Then, we investigated whether $VEGFR1^+$ monocytes in blood of patients could predict PFS or OS. In pTU patients, neither $CD11b^+/CD68^+$ nor $CD11b^+/CD68^+/VEGFR1^+$ cells predicted PFS (Fig. 5A and B) or OS (Fig. 5C and D). Also, we observed no

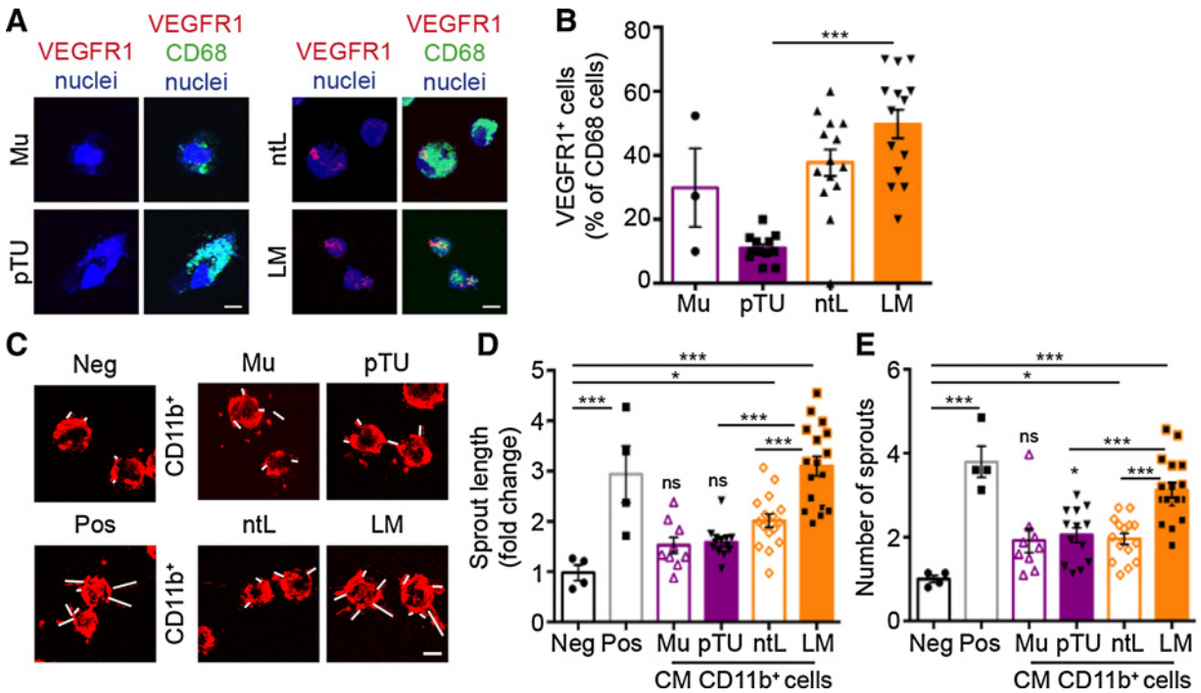

Figure 4.

Human CD11b$^+$-isolated MAMs express VEGFR1 and are proangiogenic. **A,** CD11b$^+$ cells from pTU, surrounding mucosa (Mu), liver metastasis (LM), and no tumor liver (ntL) were stained for CD68 (macrophage marker) and VEGFR1. Nuclei were counterstained with Topro-3. **B,** Quantification of the number of VEGFR1$^+$ macrophages as in **A**; (Mu, $n = 3$; pTU, $n = 12$; ntL, $n = 14$; liver metastasis, $n = 14$; one-way ANOVA; ***, $P < 0.001$). **C,** Representative images of sprouting assays analyzing the angiogenic potential of human TAMs and MAMs. CD11b$^+$ cells isolated from pTU, the surrounding "no tumor" mucosa (Mu), liver metastasis and the surrounding "no tumor" liver (ntL) were used to produce CM to stimulate endothelial cells. Starvation medium was used as negative control (Neg) and VEGF (50 ng/mL) as a positive control (Pos). Quantification of the sprout length (**D**) and the number of sprouts (**E**) showing that the CM from the liver metastasis cells induces more sprouting than the other groups (Mu, $n = 9$; pTU, $n = 13$; ntL, $n = 16$; liver metastasis, $n = 17$; one-way ANOVA; *, $P < 0.05$; ***, $P < 0.001$; ns: not significant). Scale bars, (**A** and **C**) 10 μm.

association with numbers of circulating cells and the different clinical and pathologic variables. Conversely, high percentage of CD11b$^+$/CD68$^+$ (Fig. 5E) and CD11b$^+$/CD68$^+$/VEGFR1$^+$ (Fig. 5F) circulating monocytes predicted reduced PFS in patients with liver metastasis, however not OS (Fig. 5G and H). Interestingly, high percentage of circulating VEGFR1$^+$ cells associated with clinical and pathologic variables in patients with liver metastasis (Supplementary Table S4). This group included more patients with high risk MSKCC clinical score ($P = 0.03$), with more than one liver metastasis ($P < 0.001$) and that had received neoadjuvant therapy ($P = 0.01$; Supplementary Table S4).

Thus, to determine the relevance of circulating VEGFR1$^+$ monocytes for PFS, we first investigated the general clinical and pathologic variables associated with PFS in liver metastasis (Supplementary Table S5). These analyses revealed that high MSKCC clinical risk score [HR, 1.682; 95% confidence interval (CI), 1.010–2.802; $P = 0.046$] and high number of VEGFR1$^+$-circulating macrophages (HR, 2.542; 95% CI, 1.472–4.390; $P = 0.001$) were associated with an unfavorable prognosis. To address the dependency of our variable, we next performed a multivariate Cox proportional hazard analysis with the variables associated to VEGFR1$^+$ macrophages and PFS (Supplementary Table S6). A high number of circulating VEGFR1$^+$ macrophages was an independent prognostic factor for early disease recurrence in patients with liver metastasis (HR, 2.129; 95% CI, 1.153–3.932; $P = 0.016$; Supplementary Table S6).

Taken together, our results suggest that detection of VEGFR1$^+$ monocytes in blood of patients can be a promising marker to predict disease recurrence on liquid biopsies of patients with liver metastasis.

Circulating VEGFR1$^+$ monocytes from patients with liver metastasis predict site of disease recurrence

Before metastasis, a favorable soil for cancer cells to seed and grow is formed at distant sites, as a premetastatic niche. VEGFR1$^+$ macrophages have been suggested to immunomodulate this niche to support growth of the upcoming tumor cells (14). We observed that high levels of VEGFR1$^+$-circulating monocytes predicted independently PFS as well as recurrence (Fig. 5I). Interestingly, patients in the high VEGFR1$^+$ group had more frequently a recurrence in the liver (Fig. 5I).

Considering this, the number of VEGFR1$^+$-circulating macrophages may be considered as a novel biomarker for future recurrence of metastasis in the liver.

Discussion

In this study we elucidated the role of MAMs. We found macrophage infiltration to correlate with vessel density only in liver metastases and not in pTU of patients with colorectal cancer. Also, we identified TAMs to be more M1-like and MAMs more M2-like and more proangiogenic. Both in mice and humans, we

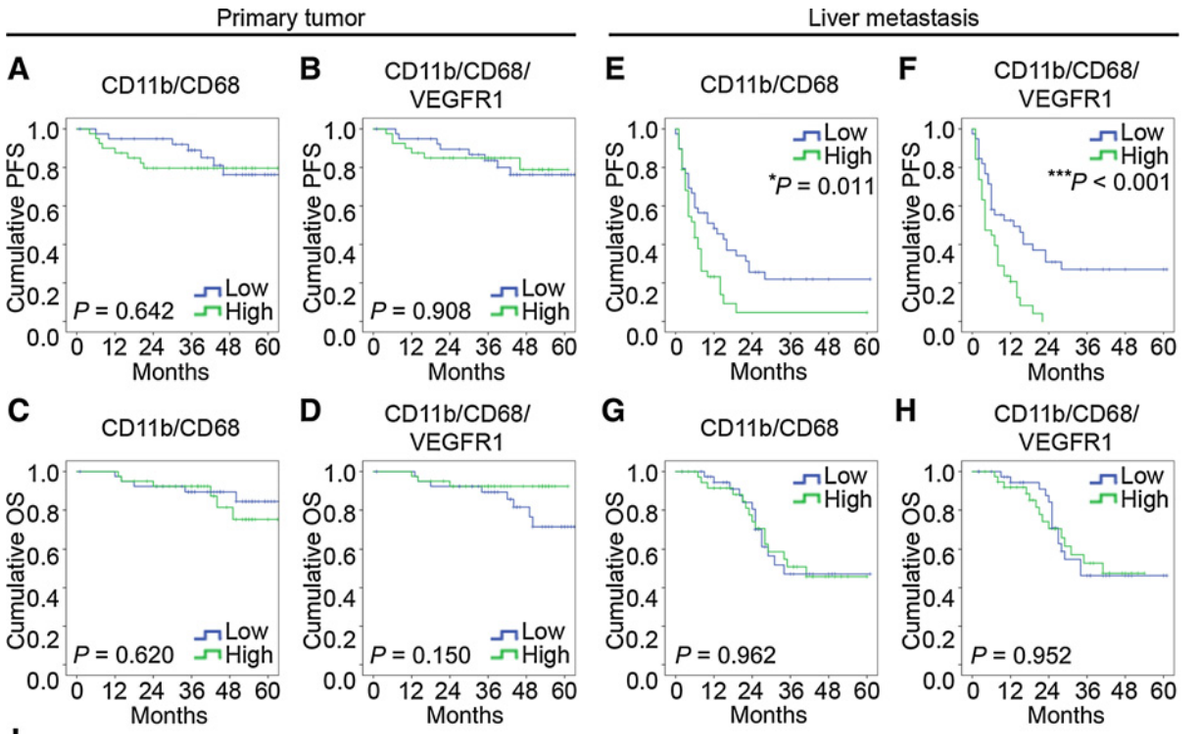

I

	Low *n* (%)	High *n* (%)	*P* value*
No. of patients	39 (100)	38 (100)	-
Recurrence			
Yes	26 (66.7)	35 (92.1)	**0.006**
No	13 (33.3)	3 (7.9)	

* Pearson test

Site of recurrence	Low *n* (%)	High *n* (%)	*P* value*
No. of patients	26 (100)	35 (100)	
Liver			
Yes	15 (57.7)	29 (82.9)	**0.030**
No	11 (42.3)	6 (17.1)	
Lung			
Yes	10 (38.5)	12 (34.3)	0.737
No	16 (61.5)	23 (65.7)	

* Pearson test.

Figure 5.

Circulating VEGFR1$^+$ monocytes predict PFS and site of recurrence in patients with liver metastasis of colorectal cancer. Kaplan–Meier curves showing PFS of pTU patients according to high ($n = 40$) or low ($n = 40$) levels of circulating CD11b$^+$/CD68$^+$ cells (**A**) and CD11b$^+$/CD68$^+$/VEGFR1$^+$ monocytes (**B**). **C** and **D,** Kaplan–Meier curves showing OS as in **A** and **B**. Kaplan—Meier curves showing PFS of patients with liver metastasis according to high ($n = 38$) or low ($n = 39$) levels of circulating CD11b$^+$/CD68$^+$ (**E**) and CD11b$^+$/CD68$^+$/VEGFR1$^+$ monocytes (**F**). **G** and **H,** Kaplan–Meier curves showing OS as in **E** and **F**. For all survival curves log-rank *P* value is shown. **I,** Association of circulating CD11b$^+$/CD68$^+$/VEGFR1$^+$ cells with site of disease recurrence in patients with liver metastasis. CD11b$^+$/CD68$^+$/VEGFR1$^+$ low < 7.26%; high >7.26% of alive cells.

found VEGFR1 expression in a subset of MAMs, which *in vivo* support angiogenesis and metastatic growth. High number of VEGFR1$^+$ cells in liver metastasis predicted reduced PFS in tissue and blood samples. Notably, circulating VEGFR1$^+$ monocytes also predicted intrahepatic recurrence in patients with liver metastasis.

Even though macrophages are involved in almost every step of tumor and metastasis progression (3, 8), little is known about their specific role and influence within metastases. Distinctive tumor microenvironments can differently activate macrophages (4) and in colorectal cancer, different microenvironments in the pTU and liver metastasis have been described previously (5, 28). Therefore, we hypothesized that TAMs and MAMs are differently polarized. In line with the literature (5, 29), in a clinically relevant mouse model of liver metastasis we observed higher infiltration of M1-like TAMs in the pTU, while, more M2-like MAMs were found in liver metastasis. The more M1-like polarization in the pTU can be explained by the inflammatory environment induced by commensal- and pathogen-derived molecules in the gut (5). On the contrary, when metastasis grows in the liver, the immunosuppressive environment supports the observed shift toward an M2-like phenotype (28).

Apart from being more M2-like polarized, in mice, we were able to identify Flt1^{hi} MAMs as a subset of macrophages, which strongly induces angiogenesis and supports metastasis growth in liver metastasis. In line with our results, Flt1$^+$ signaling in bone marrow–derived myeloid cells is necessary to induce the angiogenic response in gliomas (25). Moreover, in lung, pancreatic, and breast cancer models it was shown that Flt1 signaling in TAMs was necessary to support tumor angiogenesis (30). It has also been

reported that knockout of VEGFR1 might alter the bone marrow–derived cell infiltration into lung metastasis but not their growth, while others have shown that VEGFR1 is required for metastasis progression (31). In addition, CD11b myeloid cells expressing VEGFR1 were shown to accumulate at the premetastatic niche before the arrival of lung cancer and melanoma cells (14). On the other hand, in a mouse model of intrasplenic injection of CMT93 colorectal cancer cells, Flt1$^+$ MAMs could not be detected in the liver metastasis (32). In this tumor model, no pTU is implanted and thus, there are no metastases *per se*. Cells rapidly form intrahepatic tumor lesions within 7 days, while in our mouse model the first liver metastasis was observed after 15 days of pTU implantation. Our results support the idea that in colorectal cancer, VEGFR1$^+$ cells support metastasis and highlight the importance of adequate mouse models to study metastasis.

In human colorectal cancer primary tumors, discrepancies exist about whether or not macrophages play a role in predicting OS and/or PFS (33). In our study, we found no value for OS or PFS prediction in pTU, while others observed that the density of macrophage infiltration inversely correlates with patients' survival (34). Our results from the murine model support the notion that in pTU, M1-like TAMs can account for the benefit in OS observed in other studies (35, 36), and that discriminating TAM subpopulations is needed to better understand the overall impact of macrophage infiltration on patient outcome. Not only the plasticity of macrophages within the microenvironment could explain these differences (4, 24) but also, analysis of different tumor areas like the invasive front (35) or the whole tumor, as we did in this study, could contribute to these discrepancies. In line with the literature (37), we found that the bulk of CD68$^+$ macrophages predicted reduced PFS in liver metastasis.

As angiogenesis is a hallmark of cancer (8) and macrophages can support tumor angiogenesis (7), their role in metastatic angiogenesis was of high interest. In colorectal cancer it has been described that high vascular density, as a marker for tumor angiogenesis, negatively influences patient outcome both in the pTU (38) and liver metastasis (39). In our cohort of patients, this hold true for the patients with liver metastasis regarding PFS.

Here, for the first time, we observed a positive relationship between macrophages and vessel density in samples from patients with liver metastasis. Albeit TAMs of colorectal cancer are known to secrete VEGF and thereby promote angiogenesis (40), no association was found in the pTU. In line with our results, Lackner and colleagues (41) also observed no correlation between CD68$^+$ macrophages and microvessel density in colorectal cancer stage II and III pTU. This altogether indicates that macrophages in the pTU and the liver metastasis are different, in terms of their angiogenic potential.

Interestingly, our results show that also in human colorectal cancer, MAMs are more angiogenic than TAMs and that VEGFR1$^+$ MAMs are a specific angiogenic subgroup. Importantly, here we show that VEGFR1-expressing macrophages not only induce angiogenesis in liver metastasis, but also predict poor prognosis while not affecting prognosis in pTU. High protein levels of VEGFR1 in the pTU were described to either have no association with patient survival (42), supporting our data, or to be associated with worse patient outcome (43). Also, presence of more VEGFR1$^+$ cells in human liver metastasis was reported compared with colon mucosa and pTU (44). Moreover, in other tumor entities, VEGFR1 has been reported as a prognostic marker: for example, in glioma, overexpression of VEGFR1 was associated with poor prognosis (45) and in breast cancer, high VEGFR1 in the stroma correlated with worse OS (46); but to the best of our knowledge, the prognostic value of VEGFR1$^+$ cells in liver metastasis was so far not assessed.

Many efforts have been made to establish noninvasive methods to assess patient risk profiles before surgical tumor resection. In this regard, circulating tumor cells are promising candidates, but measuring them in patient-derived blood has not yet proven its practicability in clinical use (47). In line with the literature (48), our results suggest that detection of VEGFR1$^+$-circulating monocytes in the blood of patients with liver metastasis could be a promising new biomarker for recurrence of liver metastasis. Further validation will be necessary to determine its specificity. We believe that this could be a good addition to the so-called liquid biopsies for colorectal cancer.

As we observed that circulating VEGFR1$^+$ monocytes associate with neoadjuvant therapy, it will be important to find out how chemotherapy affects VEGFR1 expression. As plasma soluble VEGFR1 levels were proposed to be good biomarkers for response to neoadjuvant therapy in patients with localized rectal cancer (49), it would also be interesting to understand whether VEGFR1-circulating cells can predict response to therapy in patients with colorectal cancer. In line, low VEGFR1 gene expression levels in metastatic colorectal cancer were predictive for prolonged OS after antiangiogenic therapy (50). Therefore, it would be noteworthy to study the possibility of VEGFR1-circulating monocytes being biomarkers for antiangiogenic therapy response.

Certainly, the importance and validity of all clinical observations are limited by the retrospective character of the analysis. However, the underlying biological mechanism was conserved both in the murine model, as well as in primary isolated cells from patients. In the future, the results should be confirmed in a prospective study.

In summary, our findings show a correlation of macrophages and vessel density in patients with colorectal cancer liver metastasis, identify a new subset of proangiogenic MAMs that express high levels of VEGFR1, and suggest circulating VEGFR1$^+$ monocytes as a new biomarker to predict disease recurrence in the liver.

Disclosure of Potential Conflicts of Interest

Thomas Schmidt reports receiving speakers bureau honoraria from Servier. No potential conflicts of interest were disclosed by the other authors.

Authors' Contributions

Conception and design: A. Freire Valls, K. Knipper, C. Ruiz de Almodovar, T. Schmidt

Development of methodology: A. Freire Valls, K. Knipper, E. Giannakouri, V. Sarachaga, Y. Shen, C. Ruiz de Almodovar, T. Schmidt

Acquisition of data (provided animals, acquired and managed patients, provided facilities, etc.): A. Freire Valls, K. Knipper, E. Giannakouri, M. Wuehrl, Y. Shen, P. Radhakrishnan, J. Klose, T. Schmidt

Analysis and interpretation of data (e.g., statistical analysis, biostatistics, computational analysis): A. Freire Valls, K. Knipper, V. Sarachaga, P. Radhakrishnan, M. Schneider, T. Schmidt

Writing, review, and/or revision of the manuscript: A. Freire Valls, K. Knipper, E. Giannakouri, V. Sarachaga, P. Radhakrishnan, A. Ulrich, M. Schneider, H.G. Augustin, C. Ruiz de Almodovar, T. Schmidt

Administrative, technical, or material support (i.e., reporting or organizing data, constructing databases): K. Knipper, E. Giannakouri, S. Hinterkopf, Y. Shen, P. Radhakrishnan, J. Klose, M. Schneider, H.G. Augustin, T. Schmidt

Study supervision: K. Knipper, T. Schmidt

Acknowledgments

We thank Heike Adler, Melanie Richter, and Benjamin Schieb for great technical support and all members of the laboratory for helpful discussions. We also thank the Flow Cytometry and FACS Core Facility at ZMBH (Heidelberg, Germany) and the Nikon Imaging Center at the University of Heidelberg. Tissues of 13 synchronous patients were provided by the National Center for Tumor Diseases (Heidelberg, Germany) in accordance with the regulations of the tissue bank and the approval of the ethics committee of Heidelberg University. This work was supported by grants from the Deutsche Forschungsgemeinschaft (SCHM 2560/3-1 to T. Schmidt and projects A2 and C5 within CRC1366 "Vascular control of organ function" - project number 39404578 to H.G. Augustin and C. Ruiz de Almodovar). T. Schmidt received funding from the Jung Foundation for Science and Research and grant support by the Heidelberg Foundation of Surgery.

The costs of publication of this article were defrayed in part by the payment of page charges. This article must therefore be hereby marked *advertisement* in accordance with 18 U.S.C. Section 1734 solely to indicate this fact.

Received July 4, 2018; revised May 14, 2019; accepted June 20, 2019; published first June 25, 2019.

References

1. Siegel RL, Miller KD, Jemal A. Cancer statistics, 2016. CA Cancer J Clin 2016;66:7–30.
2. Tomlinson JS, Jarnagin WR, DeMatteo RP, Fong Y, Kornprat P, Gonen M, et al. Actual 10-year survival after resection of colorectal liver metastases defines cure. J Clin Oncol 2007;25:4575–80.
3. Qian BZ, Pollard JW. Macrophage diversity enhances tumor progression and metastasis. Cell 2010;141:39–51.
4. Lewis CE, Pollard JW.Distinct role of macrophages in different tumor microenvironments. Cancer Res 2006;66:605–12.
5. Kratochvill F, Neale G, Haverkamp JM, Van de Velde LA, Smith AM, Kawauchi D, et al. TNF counterbalances the emergence of M2 tumor macrophages. Cell Rep 2015;12:1902–14.
6. Ong SM, Tan YC, Beretta O, Jiang D, Yeap WH, Tai JJY, et al. Macrophages in human colorectal cancer are pro-inflammatory and prime T cells towards an anti-tumour type-1 inflammatory response. Eur J Immunol 2012;42: 89–100.
7. Squadrito ML, De Palma M. Macrophage regulation of tumor angiogenesis: implications for cancer therapy. Mol Aspects Med 2011;32:123–45.
8. Hanahan D, Weinberg RA. Hallmarks of cancer: the next generation. Cell 2011;144:646–74.
9. Folkman J. Role of angiogenesis in tumor growth and metastasis. Semin Oncol 2002;29:15–8.
10. Takeda A, Stoeltzing O, Ahmad SA, Reinmuth N, Liu W, Parikh A, et al. Role of angiogenesis in the development and growth of liver metastasis. Ann Surg Oncol 2002;9:610–6.
11. Sawano A, Iwai S, Sakurai Y, Ito M, Shitara K, Nakahata T, et al. Flt-1, vascular endothelial growth factor receptor 1, is a novel cell surface marker for the lineage of monocyte-macrophages in humans. Blood 2001;97: 785–91.
12. Muramatsu M, Yamamoto S, Osawa T, Shibuya M. Vascular endothelial growth factor receptor-1 signaling promotes mobilization of macrophage lineage cells from bone marrow and stimulates solid tumor growth. Cancer Res 2010;70:8211–21.
13. Qian BZ, Zhang H, Li J, He T, Yeo EJ, Soong DYH, et al. FLT1 signaling in metastasis-associated macrophages activates an inflammatory signature that promotes breast cancer metastasis. J Exp Med 2015;212: 1433–48.
14. Kaplan RN, Riba RD, Zacharoulis S, Bramley AH, Vincent L, Costa C, et al. VEGFR1-positive haematopoietic bone marrow progenitors initiate the pre-metastatic niche. Nature 2005;438:820–7.
15. Ohkubo H, Ito Y, Minamino T, Eshima K, Kojo K, Okizaki SI, et al. VEGFR1-positive macrophages facilitate liver repair and sinusoidal reconstruction after hepatic ischemia/reperfusion injury. PLoS One 2014;9:e105533.
16. Priceman SJ, Sung JL, Shaposhnik Z, Burton JB, Torres-Collado AX, Moughon DL, et al. Targeting distinct tumor-infiltrating myeloid cells by inhibiting CSF-1 receptor: combating tumor evasion of antiangiogenic therapy. Blood 2010;115:1461–71.
17. Fong Y, Fortner J, Sun RL, Brennan MF, Blumgart LH. Clinical score for predicting recurrence after hepatic resection for metastatic colorectal cancer: analysis of 1001 consecutive cases. Ann Surg 1999;230:309–21.
18. Peng Y, Zhai Z, Li Z, Wang L, Gu J. Role of blood tumor markers in predicting metastasis and local recurrence after curative resection of colon cancer. Int J Clin Exp Med 2015;8:982–90.
19. Balachandran VP, Arora A, Gonen M, Ito H, Turcotte S, Shia J, et al. A validated prognostic multigene expression assay for overall survival in resected colorectal cancer liver metastases. Clin Cancer Res 2016;22: 2575–82.
20. Stöth M, Freire Valls A, Chen M, Hidding S, Knipper K, Shen Y, et al. Splenectomy reduces lung metastases and tumoral and metastatic niche inflammation. Int J Cancer 2019 Apr 29 [Epub ahead of print].
21. Zhang Y, Davis C, Ryan J, Janney C, Peña MMO. Development and characterization of a reliable mouse model of colorectal cancer metastasis to the liver. Clin Exp Metastasis 2013;30:903–18.
22. Schmitz R, Freire Valls A, Yerbes R, Richter S, Kahlert C, Loges S, et al. TAM receptors Tyro3 and Mer as novel targets in colorectal cancer. Oncotarget 2016;7:56355–70.
23. Wang X, Freire Valls A, Schermann G, Shen Y, Moya IM, Castro L, et al. YAP/TAZ Orchestrate VEGF signaling during developmental angiogenesis. Dev Cell 2017;42:462–78.
24. Lawrence T, Natoli G. Transcriptional regulation of macrophage polarization: enabling diversity with identity. Nat Rev Immunol 2011;11: 750–61.
25. Kerber M, Reiss Y, Wickersheim A, Jugold M, Kiessling F, Heil M, et al. Flt-1 signaling in macrophages promotes glioma growth *in vivo*. Cancer Res 2008;68:7342–51.
26. De Palma M, Venneri MA, Galli R, Sergi LS, Politi LS, Sampaolesi M, et al. Tie2 identifies a hematopoietic lineage of proangiogenic monocytes required for tumor vessel formation and a mesenchymal population of pericyte progenitors. Cancer Cell 2005;8:211–26.
27. Mouta Carreira C, Nasser SM, di Tomaso E, Padera TP, Boucher Y, Tomarev SI, et al. LYVE-1 is not restricted to the lymph vessels: expression in normal liver blood sinusoids and down-regulation in human liver cancer and cirrhosis. Cancer Res 2001;61:8079–84.
28. Brodt P. Role of the microenvironment in liver metastasis: from pre- to prometastatic niches. Clin Cancer Res 2016;22:5971–82.
29. Edin S, Wikberg ML, Dahlin AM, Rutegård J, Öberg Å, Oldenborg PA, et al. The distribution of macrophages with a M1 or M2 phenotype in relation to prognosis and the molecular characteristics of colorectal cancer. PLoS One 2012;7:e47045.
30. Casazza A, Laoui D, Wenes M, Rizzolio S, Bassani N, Mambretti M, et al. Impeding macrophage entry into hypoxic tumor areas by Sema3A/Nrp1 signaling blockade inhibits angiogenesis and restores antitumor immunity. Cancer Cell 2013;24:695–709.
31. Dawson MR, Duda DG, Fukumura D, Jain RK. VEGFR1-activity-independent metastasis formation. Nature 2009;461:E4.
32. Kitamura T, Fujishita T, Loetscher P, Revesz L, Hashida H, Kizaka-Kondoh S, et al. Inactivation of chemokine (C-C motif) receptor 1 (CCR1) suppresses colon cancer liver metastasis by blocking accumulation of immature myeloid cells in a mouse model. Proc Natl Acad Sci U S A 2010;107: 13063–8.
33. Schmidt T, Ben-Batalla I, Schultze A, Loges S. Macrophage-tumor crosstalk: role of TAMR tyrosine kinase receptors and of their ligands. Cell Mol Life Sci 2012;69:1391–414.
34. Gulubova M, Ananiev J, Yovchev Y, Julianov A, Karashmalakov A, Vlaykova T. The density of macrophages in colorectal cancer is inversely correlated to TGF-β1 expression and patients' survival. J Mol Histol 2013;44:679–92.
35. Forssell J, Öberg Å, Henriksson ML, Stenling R, Jung A, Palmqvist R. High macrophage infiltration along the tumor front correlates with improved survival in colon cancer. Clin Cancer Res 2007;13:1472–9.

36. Annika Å, Heikki I, Samuli V, Heikki H, Jari S, Marko S, et al. Type and location of tumorinfiltrating macrophages and lymphatic vessels predict survival of colorectal cancer patients. Int J Cancer 2011;131: 864–73.
37. Cavnar MJ, Turcotte S, Katz SC, Kuk D, Gönen M, Shia J, et al. Tumor-associated macrophage infiltration in colorectal cancer liver metastases is associated with better outcome. Ann Surg Oncol 2017;24: 1835–42.
38. Tanigawa N, Amaya H, Matsumura M, Lu C, Kitaoka A, Matsuyama K, et al. Tumor angiogenesis and mode of metastasis in patients with colorectal cancer. Cancer Res 1997;57:1043–6.
39. Nanashima A, Yamaguchi H, Sawai T, Yamaguchi E, Kidogawa H, Matsuo S, et al. Prognostic factors in hepatic metastases of colorectal carcinoma: immunohistochemical analysis of tumor biological factors. Dig Dis Sci 2001;46:1623–8.
40. Barbera-Guillem E, Nyhus JK, Wolford CC, Friece CR, Sampsel JW. Vascular endothelial growth factor secretion by tumor-infiltrating macrophages essentially supports tumor angiogenesis, and IgG immune complexes potentiate the process. Cancer Res 2002;62:7042–9.
41. Lackner C, Jukic Z, Tsybrovskyy O, Jatzko G, Wette V, Hoefler G, et al. Prognostic relevance of tumour-associated macrophages and von Willebrand factor-positive microvessels in colorectal cancer. Virchows Arch 2004;445:160–7.
42. Al-Maghrabi J, Gomaa W, Buhmeida A, Qari Y, Al-Qahtani M, Al-Ahwal M. Prognostic significance of VEGFR1/Flt-1 immunoexpression in colorectal carcinoma. Tumor Biol 2014;35:9045–51.
43. Huang Y, Huang Y, Liu D, Wang T, Bai G. Flt-1-positive cells are cancer-stem like cells in colorectal carcinoma. Oncotarget 2017;8:76375–84.
44. Fan F, Wey JS, McCarty MF, Belcheva A, Liu W, Bauer TW, et al. Expression and function of vascular endothelial growth factor receptor-1 on human colorectal cancer cells. Oncogene 2005;24:2647–53.
45. Phillips HS, Kharbanda S, Chen R, Forrest WF, Soriano RH, Wu TD, et al. Molecular subclasses of high-grade glioma predict prognosis, delineate a pattern of disease progression, and resemble stages in neurogenesis. Cancer Cell 2006;9:157–73.
46. Mylona E, Alexandrou P, Giannopoulou I, Liapis G, Sofia M, Keramopoulos A, et al. The prognostic value of vascular endothelial growth factors (VEGFs)-A and-B and their receptor, VEGFR-1, in invasive breast carcinoma. Gynecol Oncol 2007;104:557–63.
47. Groot Koerkamp B, Rahbari NN, Büchler MW, Koch M, Weitz J. Circulating tumor cells and prognosis of patients with resectable colorectal liver metastases or widespread metastatic colorectal cancer: a meta-analysis. Ann Surg Oncol 2013;20:2156–65.
48. Hamm A, Prenen H, Van Delm W, Di Matteo M, Wenes M, Delamarre E, et al. Tumour-educated circulating monocytes are powerful candidate biomarkers for diagnosis and disease follow-up of colorectal cancer. Gut 2015;65:990–1000.
49. Duda DG, Willett CG, Ancukiewicz M, Di Tomaso E, Shah M, Czito BG, et al. Plasma soluble VEGFR-1 is a potential dual biomarker of response and toxicity for bevacizumab with chemoradiation in locally advanced rectal cancer. Oncologist 2010;15:577–83.
50. Weickhardt AJ, Williams D, Lee C, Simes J, Murone C, Wilson K, et al. Vascular endothelial growth factors (VEGF) and VEGF receptor expression as predictive biomarkers for benefit with bevacizumab in metastatic colorectal cancer (mCRC): analysis of the phase III MAX study. J Clin Oncol 2011;29:3531.